Numerical solution of hyperbolic moment models for the Boltzmann equation

J. Koellermeier[a,*], M. Torrilhon[a]

[a] *MathCCES, RWTH Aachen University, Schinkelstr. 2, 52062 Aachen, Germany*

Abstract

The Boltzmann equation can be used to model rarefied gas flows in the transition or kinetic regime, i.e. for moderate to large Knudsen numbers. However, standard moment methods like Grad's approach lack hyperbolicity of the equations. This can lead to instabilities and nonphysical solutions. Based on recent developments in this field we have recently derived a quadrature-based moment method leading to globally hyperbolic and rotationally invariant moment equations. We present a 1D five moment case of the equations and use numerical simulations to compare the new model with standard approaches. The tests are done with dedicated numerical methods to solve the new non-conservative moment equations. These first results using the new method show the accuracy of the new method and its benefits compared with Grad's method or other existing models like discrete velocity.

Keywords: Boltzmann equation, hyperbolicity, moment method, non-conservative numerics

1. Introduction

Kinetic equations are used in many areas of application, see e.g. [5], [8], [11]. They are especially useful to model rarefied gases and to observe non-equilibrium effects of gas flows at very high velocities and temperatures. A kinetic equation like the Boltzmann equation is usually the basis of a more advanced PDE model that goes beyond the standard fluid dynamics of for example Euler or Navier-Stokes equations. The aim is to derive PDE systems that are model equations for rarefied gas dynamics. This is usually done by deriving a larger set of equations than in the Euler or Navier-Stokes case. The better approximation quality of the new model equations, which are called moment equations, unfortunately goes together with a higher computational effort when it comes to solving the equations. The reason is that there are additional variables in the model that account for the non-equilibrium behavior of the flow.

*Corresponding author

Email addresses: koellermeier@mathcces.rwth-aachen.de (J. Koellermeier), mt@mathcces.rwth-aachen.de (M. Torrilhon)

The very first approach to the derivation of moment equations has been done by Grad in 1949, see [7]. The problem with his equations is that they are not globally hyperbolic. Hyperbolicity is related to the existence of finite and real propagation speeds in the system of equations, see [9] for more information about hyperbolic moment systems. This property can be lost in certain regions of the flow, usually already at moderate non-equilibrium. See for example [2] for a derivation of the hyperbolicity region of Grad's equations in 1D. In nD the Maxwellian is in fact already on the boundary of the hyperbolicity region as shown in [3]. In numerical simulations this leads to instabilities and most certainly nonphysical solutions. The loss of hyperbolicity is considered to be a major deficiency for Grad's method and has led to relatively few research on Grad's system.

Despite the benefits of stable equations, hyperbolicity also yields some additional numerical benefits such as a generally less restrictive CFL condition at least in comparison with parabolic equations, especially on unstructured grids. A physical motivation to obtain hyperbolic equations is that the underlying physical processes like hypersonic flows are usually hyperbolic, i.e. there are bounds on the transport of information.

During the last several years this problem has been investigated in great detail and several new models have been developed that are based on a similar derivation but lead to globally hyperbolic systems of equations. The first system called Hyperbolic Moment Equations (HME) was developed by Cai et al. in [2] and extended to the multi-dimensional case in [3] and is based on a careful investigation of the characteristic polynomial of the system matrix. Shortly after that, the Quadrature-Based Projection Method was developed in [9] and extended to the multi-dimensional case in [10] and led to the proposition of another very similar moment system called the Quadrature-Based Moment Equations (QBME). Both systems are very similar even though the idea seems to be very different and the authors have since then worked on a unifying theory and just recently proposed an operator projection framework [6] that brings together both methods and even includes more general methods.

Apart from the benefits of a globally hyperbolic PDE system, the new equations pose several challenges regarding the numerical solution. The most important difficulty is the lack of a conservation form. Even though the conservation laws of mass, momentum and energy can be fully recovered, it is no longer possible to write the higher order equations in conservation form. This makes the numerical solution much more difficult as a standard flux-based Finite Volume method is no longer applicable and more dedicated numerical methods have to be applied. However, the numerical scheme should still guarantee conservation of mass, momentum and energy.

It is the purpose of this paper to describe the first successful numerical solution of the QBME system. After a short introduction, we briefly describe the derivation of the method and compare a special 1D five moment case with the existing HME and Grad's approach. We will then present a shock-tube test case where we compute a numerical solution using the PRICE-C algorithm of Canestrelli [4] and again compare with the other models as well as with a

discrete velocity reference solution. The paper ends with concluding remarks.

2. A transformed Boltzmann equation

In kinetic theory the evolution of the mass density function $f(t, \boldsymbol{x}, \boldsymbol{c})$ is described by the Boltzmann Transport Equation

$$\frac{\partial}{\partial t} f(t, \boldsymbol{x}, \boldsymbol{c}) + c_i \frac{\partial}{\partial x_i} f(t, \boldsymbol{x}, \boldsymbol{c}) = S(f), \tag{1}$$

where we consider a d-dimensional setting, i.e. we have position $\boldsymbol{x} \in \mathbb{R}^d$, microscopic velocity $\boldsymbol{c} \in \mathbb{R}^d$ and velocity $\boldsymbol{u} \in \mathbb{R}^d$. Note that we use index notation, whenever the indices are no further specified, e.g. in the transport term of Equation (1). As we focus on the transport part of Equation (1), we first neglect the right-hand side collision operator $S(f)$. However, models for the right-hand side exist and in the test Section 6 we will later use a BGK-type model [1] to approximate the collision term.

The distribution function $f(t, \boldsymbol{x}, \boldsymbol{c})$ is related to the macroscopic quantities density ρ, velocity $\boldsymbol{u}$ and temperature θ via integration over the velocity space as follows:

$$\rho(t, \boldsymbol{x}) = \int_{\mathbb{R}^d} f(t, \boldsymbol{x}, \boldsymbol{c}) \, d\boldsymbol{c}, \tag{2}$$

$$\rho(t, \boldsymbol{x}) \boldsymbol{u}(t, \boldsymbol{x}) = \int_{\mathbb{R}^d} \boldsymbol{c} f(t, \boldsymbol{x}, \boldsymbol{c}) \, d\boldsymbol{c}, \tag{3}$$

$$d \cdot \rho(t, \boldsymbol{x}) \theta(t, \boldsymbol{x}) = \int_{\mathbb{R}^d} |\boldsymbol{c} - \boldsymbol{u}|^2 f(t, \boldsymbol{x}, \boldsymbol{c}) \, d\boldsymbol{c}. \tag{4}$$

The mathematical task is now to derive model equations for the macroscopic quantities that go beyond the standard fluid dynamics equations. One is usually not interested in the actual function f as the macroscopic quantities are of more physical relevance.

A very simple system of equations for these macroscopic variables can be derived by multiplication of Equation (1) with monomials $\left(1, \boldsymbol{c}, c^2\right)$ and subsequent integration over the velocity space. The emerging equations are the conservation laws of mass, momentum and energy, see e.g. [12].

To derive more advanced models, we need to propose an ansatz for the distribution function. In order to be more accurate, we include the macroscopic variables in the ansatz, which can also be interpreted as a transformation of the equation. We apply a nonlinear transformation of the velocity variable in order to obtain a Lagrangian velocity phase space and exhibit physical adaptivity, which allows for efficient and yet simple discretizations according to [9]:

$$\boldsymbol{\xi}(t, \boldsymbol{x}, \boldsymbol{c}) := \frac{\boldsymbol{c} - \boldsymbol{u}(t, \boldsymbol{x})}{\sqrt{\theta(t, \boldsymbol{x})}}, \tag{5}$$

such that the distribution function can be written as

$$f(t, \boldsymbol{x}, \boldsymbol{\xi}) = f\left(t, \boldsymbol{x}, \frac{\boldsymbol{c} - \boldsymbol{u}(t, \boldsymbol{x})}{\sqrt{\theta(t, \boldsymbol{x})}}\right). \tag{6}$$

This yields a shift of the microscopic velocity $\boldsymbol{c}$ by the mean velocity $\boldsymbol{u}$ and a scaling by the temperature θ, see also Fig. 1 for the effect of this transformation on two one-dimensional Gaussians. The benefit of the transformation is an easier subsequent discretization. We can later simply use the transformed velocity variable ξ for the discretization in velocity space. As a 1D example the simple choice of five centered Gauss-Hermite quadrature points leads to an accurate approximation of both Gaussians due to the adaptive transformation of the quadrature points as can be seen in Fig. 1. Note that a fixed quadrature grid would need many more points to accurately capture the distribution function for varying velocities and temperatures.

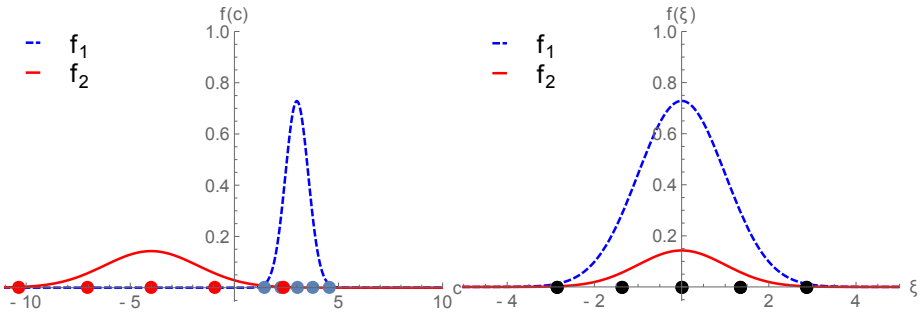

(a) untransformed Gaussians, depending on c (b) transformed Gaussians, depending on ξ

Figure 1: 1D Gaussians f_1 with $\rho_1 = 1$, $u_1 = 3$, $\theta_1 = 0.3$ and f_2 with $\rho_2 = 0.8$, $u_2 = -4$, $\theta_2 = 5$. One set of discrete sampling points in (b) equals two adaptive sets of points in (a).

3. Velocity space discretization

The velocity discretization can be done in a multi-dimensional setting as described in [3]. However, as our test case will be one-dimensional, we will for simplicity only describe the 1D velocity discretization here.

We expand the distribution function in a series of basis functions times coefficients around local equilibrium

$$f(t, x, \xi) = \sum_{\alpha=0}^{M} f_\alpha(t, x) H_\alpha(\xi), \tag{7}$$

using weighted Hermite basis functions in the transformed velocity variable ξ defined as

$$H_\alpha(\xi) = \frac{1}{\sqrt{2\pi}}\theta^{-\frac{\alpha+1}{2}} He_\alpha(\xi) \exp\left(-\frac{\xi^2}{2}\right), \tag{8}$$

for standard Hermite polynomials He_α of degree $\alpha \in \mathbb{N}$.

Using the ansatz (7) it is now possible to multiply the transformed Boltzmann equation with test functions and integrate over velocity space to end up with a PDE in space and time with reduced dimension. This system of PDEs is called a moment system, because one is taking the moments of the Boltzmann equation.

There exist different moment models and we will explain some of them which are using the ansatz from above in a 1D setting.

4. Hyperbolic models using operator projection

A straightforward procedure to derive moment equations is to multiply Equation (1) including the inserted transformations (5) and the ansatz (7) with test functions, for example the basis functions themselves, and integrate over the whole velocity space. This is known as projection of the equation on the test functions. However, standard projection methods like Grad [7] do not lead to hyperbolic PDE systems. This has been proven in many previous papers, see for example [2]. The reason for the loss of hyperbolicity seem to be the additional terms introduced by the adaptive velocity shift. As explained before, hyperbolicity is necessary for physical solutions and stability of the simulation.

Recently, different methods have been developed to derive globally hyperbolic systems. The first method leads to the Hyperbolic Moment Equations (HME) by Cai et al. [3]. Another new method yields the Quadrature-Based Moment Equations (QBME) by Koellermeier et al. [10]. The methods can be derived in the same framework. Here we want to give a 1D example of QBME and compare to HME and Grad's approach.

The Quadrature-Based Moment Equations can be explained using three different approaches: The first approach is to substitute the exact integration over velocity space by Gaussian quadrature formulas, see [10] for details, which changes some terms as the quadrature is not exact for all occurring terms. On the other hand, it is also possible to cut off higher order terms several times during the derivation of the equation system which is equivalent to using a quadrature formula. The same result can be obtained by repeated projection of the equations onto a subspace during the derivation, which is a more general approach. For details on the projection approach, we would like to refer the reader to [6].

Due to the similar derivation, the different models Grad, HME and QBME are actually very similar and only differ in some terms of the higher order equations. The rest of the equations is the same, especially the first equations including the conservation laws.

5. A 1D five moment example

As an example of the moment equations, we want to show the 1D five moment case. This case is especially important as it corresponds to the 13 moment case in 3D and is the smallest test case including heat flux and stress tensor.

We denote the right hand side collision term as $\boldsymbol{S}(\boldsymbol{u})$. An explicit example for $\boldsymbol{S}(\boldsymbol{u})$ will be explained in the next section. It is important to note that the right hand side will always have the same form for all our models and thus does not depend on the projection process.

We write the different models in the following form to allow for comparison:

$$\partial_t \boldsymbol{u}_M + \boldsymbol{A}\partial_x \boldsymbol{u}_M = \boldsymbol{S}(\boldsymbol{u}), \tag{9}$$

where only the system matrix $\boldsymbol{A}$ depends on the model. We can analytically derive this matrix for arbitrary M, but here we consider a 1D five moment case, so it is $M = 4$. For the variable vector $\boldsymbol{u}_4 = (\rho, u, \theta, f_3, f_4)$ the Grad model results in the following system matrix:

$$\boldsymbol{A}_{\text{Grad}} = \begin{pmatrix} u & \rho & 0 & 0 & 0 \\ \frac{\theta}{\rho} & u & 1 & 0 & 0 \\ 0 & 2\theta & u & \frac{6}{\rho} & 0 \\ 0 & 4f_3 & \frac{\rho\theta}{2} & u & 4 \\ -\frac{f_3\theta}{\rho} & 5f_4 & \frac{3f_3}{2} & \theta & u \end{pmatrix}. \tag{10}$$

For this system matrix, the hyperbolicity can be analyzed by computing the eigenvalues and checking whether the eigenvalues are all real. In Grad's model, the eigenvalues depend on the higher order variables f_3, f_4 and imaginary eigenvalues correspond to a loss of hyperbolicity as analyzed in [2]. This already occurs for moderate values of the higher order non-equilibrium basis coefficients in the expansion (7) as can be seen in Figure 2 where the hyperbolicity region is colored in blue depending on the scaled variables $\widetilde{f}_3 = \frac{f_3}{\rho\theta^{3/2}}$ and $\widetilde{f}_4 = \frac{f_4}{\rho\theta^2}$.

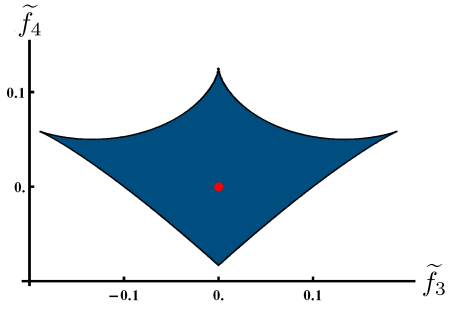

Figure 2: Hyperbolicity region of Grad's method for $M = 4$.

The new moment models are all globally hyperbolic and yield the following

system matrices.

$$\boldsymbol{A}_{\mathrm{HME}} = \begin{pmatrix} u & \rho & 0 & 0 & 0 \\ \frac{\theta}{\rho} & u & 1 & 0 & 0 \\ 0 & 2\theta & u & \frac{6}{\rho} & 0 \\ 0 & 4f_3 & \frac{\rho\theta}{2} & u & 4 \\ -\frac{f_3\theta}{\rho} & 0 & -f_3 & \theta & u \end{pmatrix}, \tag{11}$$

$$\boldsymbol{A}_{\mathrm{QBME}} = \begin{pmatrix} u & \rho & 0 & 0 & 0 \\ \frac{\theta}{\rho} & u & 1 & 0 & 0 \\ 0 & 2\theta & u & \frac{6}{\rho} & 0 \\ 0 & 4f_3 & \frac{\rho\theta}{2} - \frac{10f_4}{\theta} & u & 4 \\ -\frac{f_3\theta}{\rho} & 5f_4 & -f_3 & \theta + \frac{15f_4}{\rho\theta} & u \end{pmatrix}, \tag{12}$$

where terms written in red represent changes with respect to the standard Grad model that originate from the operator projection procedure, see also [6]. Other models with $M > 4$ have the same structure and also only differ from the Grad model in some entries of the last equations, the same is valid for the multi-dimensional case.

The changed entries in Equations (11) and (12) are not arbitrary but chosen in a special way to guarantee global hyperbolicity while keeping as much as possible of the original system including the first three equations which correspond to the conservation laws of mass, momentum and energy. In the case of HME the system is the only possibility that achieves hyperbolicity while only changing the last equation, see [2]. In the case of QBME the system results from the application of a Gaussian quadrature rule of maximum degree of exactness that only differs from the exact integration in the three entries marked in (12). For more details about the derivation we refer the reader to [9].

It is important to note that these small changes in the last equations suffice to make the equation system globally hyperbolic. In both cases it can be shown that the eigenvalues of the HME and the QBME system are in fact the same and are all finite and real.

6. Numerical simulation of a shock tube

In order to test our equation systems, we consider the following shock tube problem:

$$\partial_t \boldsymbol{u}_M + \boldsymbol{A}\partial_x \boldsymbol{u}_M = -\frac{1}{\tau}\boldsymbol{P}\boldsymbol{u}_M, \tag{13}$$

$$\boldsymbol{u}_M = \begin{cases} \boldsymbol{u}_M^L & \text{if } x < 0 \\ \boldsymbol{u}_M^R & \text{if } x > 0, \end{cases} \tag{14}$$

where the collisions have been modelled using a BGK operator with relaxation time $\tau = \frac{\mathrm{Kn}}{\rho}$, which leads to the following form of the matrix $\boldsymbol{P}$ after the projections

$$\boldsymbol{P} = \mathrm{diag}\,(0, 0, 0, 1, \ldots, 1) \tag{15}$$

for the variable vector $\boldsymbol{u}_M = (\rho, u, \theta, f_3, \ldots, f_M)\,,\ M \geq 4$. In the special case $M = 4$ the matrix $\boldsymbol{A}$ can be directly substituted by one of the model matrices $\boldsymbol{A}_{\text{Grad}}$, $\boldsymbol{A}_{\text{HME}}$ or $\boldsymbol{A}_{\text{QBME}}$ from Section 5.

According to the tests by Cai et al. [2] the left and right states are chosen as

$$\boldsymbol{u}_M^L = (7, 0, 1, 0, \ldots, 0)^T\,, \qquad \boldsymbol{u}_M^R = (1, 0, 1, 0, \ldots, 0)^T\,, \tag{16}$$

corresponding to a jump in density at the discontinuity at $x = 0$. We therefore expect a rarefaction wave travelling to the left, a contact discontinuity travelling right and a faster shock wave also travelling right in front of the contact discontinuity.

The systems (9) as well as (13) are clearly not in conservation form. It turns out that in fact both the HME and QBME model cannot be written in conservation form. For the solution of the equations special numerical methods have to be used as a standard flux-based Finite Volume scheme is not applicable. In this first test we will use the PRICE-C scheme of Canestrelli [4] to discretize the non-conservative products of the equations. The reason for this choice is the possibility for an extension to higher order or to the multi-dimensional case in subsequent work. Furthermore the scheme has been successfully tested for different non-conservative equations, see e.g. [4]. As the non-conservative products only appear in the last equations and the shocks are not too strong, we expect a path-conservative numerical scheme like PRICE-C to give accurate results for our test case. Some comparison tests with a non-conservative variant of the Lax-Friedrichs method showed only slightly more diffusion in the solution and no systematic errors that can be attributed to the non-conservative form of the equations. However, different conditions might require a more detailed investigation regarding the influence of the numerical scheme.

For the numerical tests, we consider two cases $\text{Kn} = 0.05$ and $\text{Kn} = 0.5$ and run the simulation starting at $t = 0$ until $t = 0.3$ with a time step size of $\Delta t = 0.0001$ according to a CFL number of approximately 0.45. For this numerical benchmark problem, the Knudsen number changes the influence of the collision operator on the right hand side. With increasing Knudsen number the collision operator has less influence. The solution for a larger Knudsen number is in fact equivalent to the solution of the same system with smaller Knudsen number and proper scaling in the x-direction at an earlier time.

In general, we can say that our simulation results agree very well with the simulations carried out by Cai et al. in [2] where they also compared with a kinetic solver.

The test case with $\text{Kn} = 0.05$ is done with all three models, i.e. Grad, HME, QBME and a discrete velcocity model (DVM) for comparison. The results are shown in Figure 3. Besides the good agreement with the DVM solution for all methods, we can compare the new models to the existing Grad model. We see only very small differences in the values of ρ, p and u. However, some deviations from Grad's results can be seen in the right half of the domain for $x > 0$, as the initial difference in density leads to a much larger relaxation time, which makes the differences between all methods more visible. Also the

non-equilibrium variables f_3 and f_4 are very similar, despite their smaller scale. Again the deviations from Grad's results are more obvious in the region with lower density due to the larger relaxation time. Comparing HME and QBME for this Knudsen number yields almost no difference, which is also because of the large effect of the collision operator on the right hand side for Kn = 0.05. In fact, the difference between Grad and HME is only slightly smaller than the difference between Grad and QBME except for the last variable f_4 where QBME is closer to Grad's solution than HME.

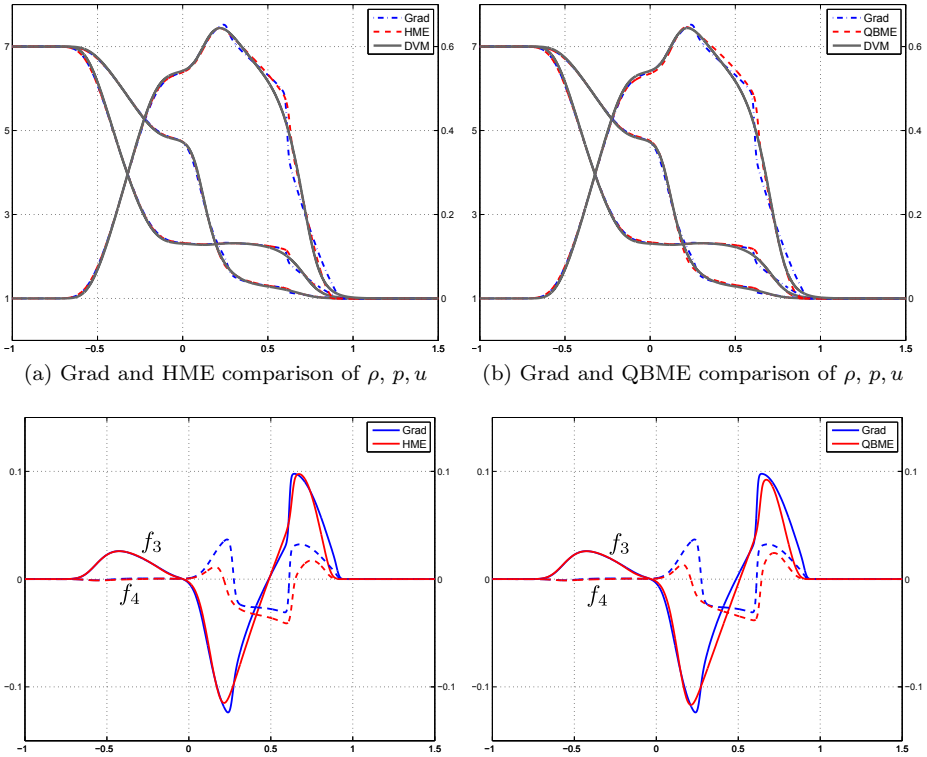

(a) Grad and HME comparison of ρ, p, u

(b) Grad and QBME comparison of ρ, p, u

(c) Grad and HME comparison of f_3 and f_4

(d) Grad and QBME comparison of f_3 and f_4

Figure 3: Numerical results of the shock tube problem for Kn = 0.05. In Figure 3a and Figure 3b the left y-axis is for ρ and p and the right axis is for u.

The test case Kn = 0.5 in Figure 4 is more interesting and also more difficult for standard methods, as the influence of the collision term on the right hand side is much smaller which makes differences in the transport part of the equations appear much earlier. A very important consequence is the effect on the stability of the methods. Even in the case Kn = 0.05 Grad's equations were at the edge of the hyperbolicity region, but now for Kn = 0.5 the state vector leaves the region of hyperbolicity and the small effects of the collision operator do not suffice to keep the stability of the computation. In our simulations the computation broke

down after a relatively small number of time steps for Grad's method due to this instability. This is why we do not show a comparison with Grad's method. HME and QBME, however, are globally hyperbolic and thus always yield stable results. The hyperbolic models HME and QBME obviously do not give a very good approximation to the DVM model, as they use far less variables to simulate the same physics. One way to achieve a better accuracy of the models with respect to the DVM solution would be to increase the number of equations of the moment models similar to [3]. However, in our work we want to consider the 5-moment case only and take a closer look at the differences between the moment models themselves. As can be seen in Figure 4, the differences are again more visible in the region where we have $x > 0$. Deviations can be seen in front of the first density shock wave at approximately $x = 0.6$ as well as in the maximum value of the velocity right at the contact discontinuity around $x = 0.2$. The differences are due to the changes in the equations as shown in Section 5. According to the smaller scale, the comparison of the higher order coefficients f_3 and f_4 shows larger differences which are most obvious at the different minima and maxima of the variables. As before, the differences are amplified in the region of smaller density due to the larger relaxation time. Note that the positions of the maxima as well as the positions of the shocks are almost the same as the eigenvalues of both the HME and the QBME system are equal.

To allow for a quantitative comparison of the models, we compute the L_1 error on the whole domain $[x_L, x_R] = [-1, 1.5]$ for the different hyperbolic moment models and variables ρ, u, p, θ. In case of the density ρ, the error is computed using

$$\epsilon_{\rho,\text{model}} = \frac{\|\rho_{\text{model}} - \rho_{\text{DVM}}\|_{L_1}}{\|\rho_{\text{DVM}}\|_{L_1}} \tag{17}$$

and similarly for the other variables.

The resulting relative errors for the test case with Kn = 0.05 are shown in Table 1. First of all we see that all errors are reasonably small. The velocity

Table 1: Relative L_1 errors for moment models. Kn = 0.05.

	ρ	u	p	θ
Grad	0.29%	1.16%	0.24%	0.64%
HME	0.15%	1.01%	0.22%	0.41%
QBME	0.24%	1.54%	0.27%	0.67%

error is relatively large which is due to the small norm $\|u_{\text{DVM}}\|_{L_1}$. Furthermore, all new hyperbolic models give a smaller error than the standard Grad method with smaller errors for the HME method.

The errors for the test case with larger Knudsen number Kn = 0.5 are shown in Table 2. Note that Grad's method breaks down and thus no error can be computed. For the hyperbolic methods in comparison with the previous test case, we observe overall larger error which is not surprising due to the stronger non-equilibrium and larger values of f_3 and f_4. The ratios between the errors of

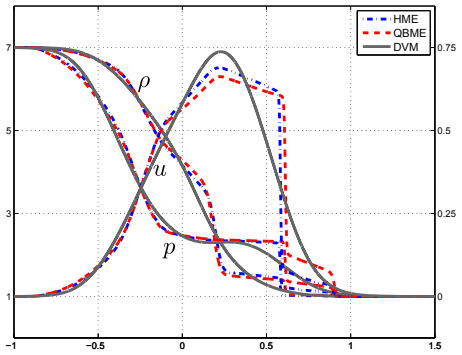

(a) HME and QBME comparison of ρ, p, u

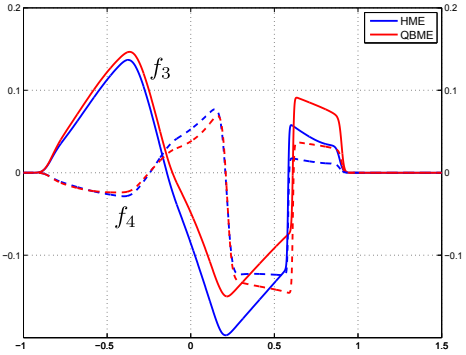

(b) HME and QBME comparison of f_3 and f_4

Figure 4: Numerical results of the shock tube problem for Kn = 0.5. Note that Grad's model breaks down for Kn = 0.5 and thus cannot be shown. In Figure 4a the left y-axis is for ρ and p and the right axis is for u.

the different variables are roughly the same when comparing Table 1 and Table 2. HME again results in slightly smaller errors than QBME which might be due to the fact that less equations are changed with respect to the original Grad model. Despite these small differences, all hyperbolic methods result in similar errors.

7. Conclusions

We have presented the Quadrature-Based Moment Equations (QBME) as a new set of globally hyperbolic equations to model rarefied gas flows. In the 1D case, the derivation is particularly easy as it only requires the application of a quadrature formula instead of exact integration. The derivation of the method can be generalized to a projection procedure, that is also applicable to many other models. In an example with the five moment case in 1D we show that

Table 2: Relative L_1 errors for moment models. Kn = 0.5.

	ρ	u	p	θ
HME	1.40%	7.50%	1.07%	2.67%
QBME	1.57%	8.74%	1.20%	4.02%

the equations are actually very similar to Grad's model and the existing HME system.

The five moment case is used to simulate a shock tube for the first time with QBME and a comparison with HME and Grad's model yields very similar results including the expected agreement with a discrete velocity model as has been shown by an error computation. An important advantage of the method with respect to Grad's system is the global hyperbolicity which allows simulations where computations with other methods become unstable.

We can see this first results as a starting point for more detailed simulation results with the new model equations and plan to perform fully two-dimensional tests as well as to apply different numerical methods for comparison in the near future.

Acknowledgements

This work has been carried out with the support of the German National Academic Foundation.

References

[1] P. L. Bhatnagar, E. P. Gross, and M. Krook. A model for collision processes in gases. *Physical Review*, 94:511–525, 1954.

[2] Z. Cai, Y. Fan, and R. Li. Globally hyperbolic regularization of Grad's moment system in one dimensional space. *Commun. Math. Sci.*, 11(2):547–571, 2013.

[3] Z. Cai, Y. Fan, and R. Li. Globally hyperbolic regularization of Grad's moment system. *Comm. Pure Appl. Math.*, 67(3):464–518, 2014.

[4] A. Canestrelli. *Numerical Modelling of Alluvial Rivers by Shock Capturing Methods*. PhD thesis, Universita' Degli Studi di Padova, 2008.

[5] R. Duclous, B. Dubroca, and M. Frank. A deterministic partial differential equation model for dose calculation in electron radiotherapy. *Phys. Med. Biol.*, 55:3843–3857, 2010.

[6] Y. Fan, J. Koellermeier, J. Li, R. Li, and M. Torrilhon. Model reduction of kinetic equations by operator projection. *J. Stat. Phys.*, 162(2):457–486, 2016.

[7] H. Grad. On the kinetic theory of rarefied gases. *Comm. Pure Appl. Math.*, 2(4):331–407, 1949.

[8] T. Kataoka, M. Tsutahara, K. Ogawa, Y. Yamamoto, M. Shoji, and Y. Sakai. Knudsen pump and its possibility of application to satellite control. *Theoretical and Applied Mechanics*, 53:155–162, 2004.

[9] J. Koellermeier. Hyperbolic approximation of kinetic equations using quadrature-based projection methods. Master's thesis, RWTH Aachen University, 2013.

[10] J. Koellermeier, R. Schaerer, and M. Torrilhon. A framework for hyperbolic approximation of kinetic equations using quadrature-based projection methods. *Kinet. Relat. Mod.*, 7(3):531–549, 2014.

[11] X. Shan and X. He. Discretization of the velocity space in the solution of the Boltzmann equation. *Physical Review Letters*, 80:65–68, 1998.

[12] H. Struchtrup. *Macroscopic Transport Equations for Rarefied Gas Flows.* Springer, 2005.